

## Layer-by-Layer Self-Assembled Chitosan/ Poly(thiophene-3-acetic acid) and Organophosphorus Hydrolase Multilayers

Celeste A. Constantine,<sup>†</sup> Sarita V. Mello,<sup>†</sup> Annie Dupont,<sup>†</sup> Xihui Cao,<sup>†</sup>  
David Santos, Jr.,<sup>‡</sup> Osvaldo N. Oliveira, Jr.,<sup>‡</sup> Francisco T. Strixino,<sup>§</sup>  
Ernesto C. Pereira,<sup>§</sup> Tu-Chen Cheng,<sup>||</sup> Joseph J. Defrank,<sup>||</sup> and Roger M. Leblanc<sup>\*,†</sup>

Contribution from the Department of Chemistry, University of Miami, 1301 Memorial Drive, Coral Gables, Florida 33146, IFSC, Universidade de Sao Paulo, C.P. 369, Sao Carlos, Sao Paulo, Brazil, CMDMC, Department of Chemistry, UFSC, 13560-970 Sao Carlos, Sao Paulo, Brazil, and Biotechnology Team, Research and Technology Directorate, U.S. Army Edgewood Chemical and Biological Center, Aberdeen Proving Ground, Maryland 21010-5423

Received September 25, 2002; E-mail: rml@miami.edu

**Abstract:** The aim of this study is to immobilize an enzyme, namely, organophosphorus hydrolase (OPH), and to detect the presence of paraoxon, which is an organophosphorus compound, using the layer-by-layer (LbL) deposition technique. To lift the OPH from the solid substrate, a pair of polyelectrolytes (positively charged chitosan (CS) and negatively charged poly(thiophene-3-acetic acid) (PTAA)) were combined. These species were made charged by altering the pH of the solutions. LbL involved alternate adsorption of the oppositely charged polyions from dilute aqueous solutions onto a hydrophilic quartz slide. This polyion cushion was held together by the electrostatic attraction between CS and PTAA. The growing process was monitored by fluorescence spectroscopy. OPH was then adsorbed onto the five-bilayer CS/PTAA system. This five-bilayer macromolecular structure compared to the solid substrate rendered stability to the enzyme by giving functional integrity in addition to the ability to react with paraoxon solutions. The ultimate goal is to use such a system to detect the presence of organophosphorus compounds with speed and sensitivity using the absorption and fluorescence detection methodologies.

### 1. Introduction

Organophosphorus (OP) derivatives are found in insecticides and pesticides that are widely used around the world.<sup>1</sup> OP compounds are structurally similar to nerve gases and act as neurotoxins by inhibiting the enzyme acetylcholinesterase, which is responsible for transmitting nerve impulses across synapses.<sup>2</sup> As a result of the acute toxicity of these OP neurotoxins, environmental monitoring of the presence of these compounds in food and groundwater is important to keep these compounds below the harmful level for humans and animals.<sup>3</sup> One such OP compound is paraoxon, which is the product of oxidative desulfuration of another pesticide, parathion.<sup>4</sup> When parathion is exposed to the atmosphere, it is converted to paraoxon, in

which the sulfur group is replaced by oxygen.<sup>5</sup> This compound is poisonous if ingested, inhaled, or absorbed through the skin.

Many analytical methods have been devised to detect the presence of OP compounds, for example, gas chromatography (GC),<sup>6,7</sup> high-performance liquid chromatography (HPLC)<sup>8,9</sup> and other electrical methods of detection.<sup>10</sup> These methods have proven to be sensitive and reliable but have significant disadvantages. They are time-consuming and expensive and must be done by skilled personnel. To overcome these disadvantages, enzymatic biosensors have been designed for speed of detection, high efficiency, and sensitivity.<sup>11</sup> The biomaterials currently in use for organophosphate detection are enzymes,<sup>12</sup> antibodies,<sup>13</sup> and cells.<sup>14</sup>

\* Corresponding author. Phone: (305) 284-2194. Fax: (305) 284-6367.

<sup>†</sup> University of Miami.

<sup>‡</sup> Universidade de Sao Paulo.

<sup>§</sup> UFSC.

<sup>||</sup> U.S. Army Edgewood Chemical Biological Center.

(1) Munnecke, D. J. *Agric. Food Chem.* **1980**, *28*, 105–111.

(2) Quinn, D. M.; Selwood, T.; Pryor, A. N.; Lee, B. H.; Leu, L. S.; Acheson, S. A.; Silman, I.; Doctor, B. P.; Rosenberry, T. L. In *Multidisciplinary Approaches to Cholinesterase Functions*; Shafferman, A., Velan, B., Eds.; Plenum Press: New York, 1992.

(3) Mulchandani, A.; Pan, S.; Chen, W. *Biotechnol. Prog.* **1999**, *15*, 130–134.

(4) *Organophosphorus Insecticides: A General Introduction*; International Programme on Chemical Safety; World Health Organization: Geneva, Finland.

(5) Boyd, M. E. In *Protein deficiency and pesticide toxicity*; Thomas, C. Ed.; Illinois, 1972.

(6) Mendoza, C. E. Thin-layer chromatography. In *Pesticide Analysis*; Dumas, K. G., Ed.; Marcel Dekker: New York, 1981, pp 1–44.

(7) Das, K. G.; Kulkarni, P. S. Gas-liquid chromatography. In *Pesticide Analysis*; Dumas, K. G., Ed.; Marcel Dekker: New York, 1981.

(8) Hanks, A. R.; Colvin, B. M. High-performance liquid chromatography. In *Pesticide Analysis*; Dumas, K. G., Ed.; Marcel Dekker: New York, 1981; pp 99–174.

(9) Barcelo, D.; Lawrence, J. F. Residue analysis of organophosphorus pesticides. In *Emerging Strategies for Pesticide Analysis*; Charins, T., Sherma, J., Eds.; CRC Press: Boca Raton, FL, 1992; pp 127–150.

(10) Palchetti, I.; Cagnini, A.; Del Carlo, M.; Coppi, C.; Mascini, M.; Turner, A. P. F. *Anal. Chim. Acta* **1997**, *337*, 315–321.

(11) Dumschat, C.; Muller, H.; Stein, K.; Schwede, G. *Anal. Chim. Acta* **1991**, *252*, 7–9.

Organophosphorus hydrolase (OPH) is an enzyme that exhibits the ability to hydrolyze a large variety of organophosphorus compounds by producing less toxic products such as *p*-nitrophenol and diethyl phosphate.<sup>15</sup> OPH selectively catalyzes a hydrolytic reaction in the P–O, P–S, P–F, and P–CN bonds in organophosphorus neurotoxins.<sup>16</sup> There are several advantages to using enzyme-based sensors, and some of these advantages are the following: rapid response times, sensitivity, and reactivation of the enzyme for continuous monitoring.<sup>17</sup> Aqueous solutions of enzymes lose their catalytic activity relatively quickly, and this activity cannot be regenerated. In lieu of this, enzymatic determination is optimized when the enzyme is immobilized. There are several methods of immobilization. Effective methods of immobilization include physical adsorption onto a solid support,<sup>18–20</sup> encapsulation into a hydrogel,<sup>21–23</sup> cross-linking,<sup>24,25</sup> and covalent binding.<sup>26–30</sup> A key requirement of enzyme immobilization is attachment without the bioactivity being sacrificed.<sup>31</sup>

The layer-by-layer deposition technique is used to generate ultrathin films with molecular order and stability. This technique overcomes some of the disadvantages of other methods of ultrathin film assembly, *vide supra*. One major advantage of this technique is that it has great industrial application in the field of biosensors. The layer-by-layer deposition method involves the alternate adsorption of oppositely charged macromolecules such as polymers and biomacromolecules.<sup>32–34</sup> This approach provides a simple method to develop films 5–500 nm thick that possess a high strength.<sup>35</sup> Owing to its simplicity and versatility different enzymes and polyions may be assembled to fabricate an ultrathin film. These have potential applications in areas such as separation or dialysis membranes,<sup>36</sup> optical devices,<sup>37</sup> and biosensors.<sup>38</sup> Electrostatic forces, covalent bonding, to a lesser extent hydrogen bonding, and hydrophobic interactions are responsible for the spontaneous assembly of these ultrathin films. The sequential adsorption of opposite

charges onto the solid substrate leads to a wide range of combinations of charged species, which can be used for self-assembled ultrathin films.<sup>39–42</sup>

In the present work, several bilayers of chitosan (CS) and poly(thiophene-3-acetic acid) (PTAA) were prepared to produce a stable supramolecular ultrathin film. CS is a high molecular weight polyglucosamine of approximately 100 kDa. CS, due to strong electrostatic segment–segment repulsion, adopts an extended conformation.<sup>43,44</sup> CS adsorbs strongly onto negatively charged surfaces, and the adsorbed CS layer adopts a flat conformation that provides a stable film on which the PTAA can be adsorbed.<sup>45</sup> PTAA has many important properties such as conductivity in the doped state,<sup>46</sup> thermochromism,<sup>47</sup> photoluminescence,<sup>48</sup> fluorescence, and absorption in the UV–vis region.<sup>49</sup> The first five bilayers offer a cushion of support and increased stability, as a result of strong electrostatic attraction between CS and PTAA due to the opposite charges. This allows for better adsorption of OPH on this cushioning support than on a solid support such as a quartz slide.<sup>50</sup> The fluorescence property of PTAA played a key role in this work as the ultrathin film was monitored using emission spectroscopy. Our methodology shows a novel way of immobilizing OPH using the alternate layer-by-layer adsorption technique. The immobilization is done under mild conditions using pH 7.3 so that the activity of OPH is not compromised. However, upon immobilization, the enzyme is stable and can be used under more harsh conditions. Layer-by-layer adsorption allows OPH to be combined with PTAA so that in the presence of paraoxon there would be a change in the optical properties of PTAA, and hence, the presence of paraoxon could be detected.

## 2. Experimental Section

**2.1. Materials and Methods.** CS was obtained from Biopolymer Engineering (Eagan, MN). A solution (1 mg/mL), pH 4.0, was prepared. PTAA was synthesized according to the published procedure.<sup>48</sup> A PTAA solution was prepared at a concentration of 1 mg/mL, using 10<sup>-1</sup> M NH<sub>4</sub>OH, and the pH was adjusted to 8.8. OPH (85–90%) (E.C. 3.1.8.1) was isolated, extracted, and purified by the U.S. Army Laboratory (Edgewood Chemical and Biological Center, Maryland). A stock solution of OPH (1.8 mg/mL) was prepared in 100 mM bis-tris–propane (BTP), pH 7.3, containing 10 μM Co<sup>2+</sup>. The stock solution was frozen at –4 °C. The stock solution was freshly thawed and diluted to a concentration of 0.18 mg/mL before use. The ionic strength of the above solutions was adjusted with NaCl. Buffers were used as washing solutions to maintain the same pH as the dipping solutions: pH 4.0 (0.1 M C<sub>8</sub>H<sub>5</sub>O<sub>4</sub>K and 0.1 M HCl), pH 8.8 (0.1 M C<sub>4</sub>H<sub>11</sub>NO<sub>3</sub> and 0.1 M HCl), pH 7.3 (0.1 M KH<sub>2</sub>PO<sub>4</sub> and 0.1 M NaOH). The water used was purified by a Modulab 2020 water purification system (Continental Water Systems Corp., San Antonio, TX). The pure water has a specific resistance of 18 MΩ·cm and a surface tension of 72.6 mN m<sup>-1</sup> at 20 ± 1 °C.

- (12) Van Emon, J. M.; Lopez-Avila, V. *Anal. Chem.* **1992**, *64*, 79–88.
- (13) Shimazu, M.; Mulchandani, A.; Chen, W. *Biotechnol. Prog.* **2001**, *17*, 76–80.
- (14) Reiner, E.; Aldridge, W. N.; Hoskin, F. C. G., Eds. *Enzymes hydrolyzing organophosphorus compounds*; Ellis Horwood, Chichester, U.K., 1989.
- (15) Munneke, D. M. *Biotechnol. Bioeng.* **1979**, *21*, 2247–2261.
- (16) Russell, R.; Pishko, M.; Simonian, A. S.; Wild, J. R. *Anal. Chem.* **1999**, *71*, 4909–4912.
- (17) Marty, J.; Leca, B.; Noguier, T. *Analisis* **1998**, *26*, 144–149.
- (18) Mesthrige, K. W.; Amro, N.; Liu, G. *Scanning* **2000**, *22*, 380–388.
- (19) Yan, A. X.; Li, X. W.; Ye, Y. H. *Appl. Biochem. Biotechnol.* **2002**, *101*, 113–129.
- (20) Lee, J. G.; Lee, W. C. *Biotechnol. Appl. Biochem.* **1998**, *27*, 225–230.
- (21) Decher, G. *Science* **1997**, *277*, 1232–1237.
- (22) Wei, Y.; Xu, J. G.; Feng, Q. W. *J. Nanosci. Nanotechnol.* **2001**, *1*, 83–93.
- (23) Wei, Y.; Xu, J. G.; Feng, Q. W. *Mater. Lett.* **2000**, *44*, 6–11.
- (24) Carbone, K.; Casarci, M.; Varrone, M. *J. Appl. Polym. Sci.* **1999**, *74*, 1881–1889.
- (25) Ulbricht, M.; Papra, A. *Enzyme Microb. Technol.* **1997**, *20*, 61–68.
- (26) Norde, W.; Zoungrana, T. *Biotechnol. Appl. Biochem.* **1998**, *28*, 133–143.
- (27) Alkorta, I.; Garbisu, C.; Llama, M. *J. Enzyme Microb. Technol.* **1996**, *18*, 141–146.
- (28) Wang, P.; Dai, S.; Waezsada, S. D. *Biotechnol. Bioeng.* **2001**, *74*, 249–255.
- (29) Chae, H.; Kim, E. *Appl. Biochem. Biotechnol.* **1998**, *73*, 195–204.
- (30) Mateo, C.; Fernandez-Lorente, G.; Abian, O. *Biomacromolecules* **2000**, *1*, 739–745.
- (31) Gill, I.; Ballesteros, A. *Trends Biotechnol.* **2000**, *15*, 282–296.
- (32) Cosnier, S. *Biosens. Bioelectron.* **1999**, *14*, 443–456.
- (33) Cordek, J.; Wang, X.; Tan, W. *Anal. Chem.* **1999**, *71*, 1529–1533.
- (34) Lvov, Y.; Decher, G.; Mohwald, H. *Langmuir* **1993**, *9*, 481–486.
- (35) Keller, S.; Kim, H.; Mallouk, T. J. *Am. Chem. Soc.* **1994**, *116*, 8817–8818.
- (36) Fabianowski, W.; Roszko, M.; Brodzinska, W. *Thin Solid Films* **1998**, *327*, 743–747.
- (37) Wagner, M.; Tamm, L. *Biophys. J.* **2000**, *79*, 1400–1414.
- (38) Serizawa, T.; Hashiguchi, S.; Akashi, M. *Langmuir* **1999**, *15*, 5363–5368.

- (39) Lvov, Y.; Yamada, S.; Kunitake, T. *Thin Solid Films* **1997**, *300*, 107–112.
- (40) Joly, S.; Kane, R.; Razilovski, L.; Wang, T.; Wu, A.; Cohen, R.; Thomas, E.; Rubner, M. *Langmuir* **2000**, *16*, 1354–1359.
- (41) Onda, M.; Ariga, K.; Kunitake, T. *J. Biosci. Bioeng.* **1999**, *87*, 69–75.
- (42) Sano, M.; Lvov, Y.; Kunitake, T. *Annu. Rev. Mater. Sci.* **1996**, *26*, 153–187.
- (43) Claesson, P.; Ninham, B. *Langmuir* **1992**, *8*, 1406–1412.
- (44) Lu, C.; Luo, C.; Cao, W. *Colloids Surf., B* **2002**, *25*, 19–27.
- (45) Hoogeveen, N.; Stuart, M.; Fleer, G. *Langmuir* **1996**, *12*, 36–39.
- (46) Leclerc, M.; Roux, C.; Bergeron, Y. *Synth. Met.* **1993**, *287*, 55–57.
- (47) Jung, S.; Hwang, D.; Zyung, T.; Kim, W.; Chittibabu, K.; Tripathy, S. *Synth. Met.* **1998**, *98*, 107–111.
- (48) Desouza, J.; Pereira, E. *Synth. Met.* **2001**, *118*, 167–170.
- (49) Ferreira, M.; Rubner, M. F. *Macromolecules* **1995**, *28*, 7107–7114.
- (50) Wagner, M. L.; Tamm, L. K. *Biophys. J.* **2000**, *79*, 1400–1414.

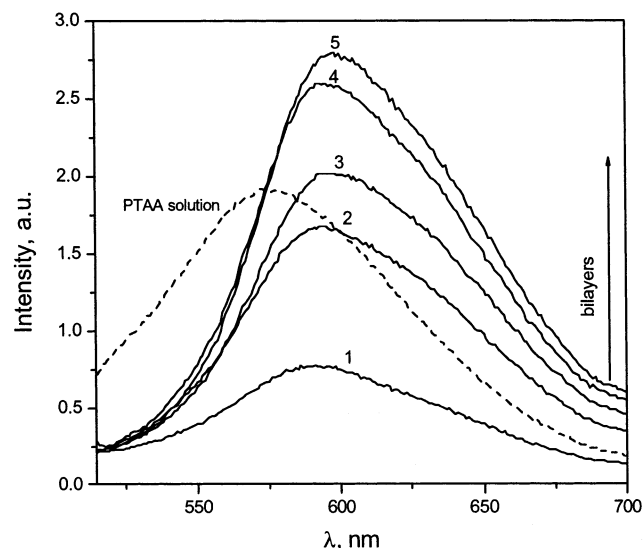


**Figure 1.** Fluorescence spectra of the PTAA solution (0.1 mg/mL) and CS/PTAA binary system deposited onto the hydrophilic quartz slide used to confirm the CS/PTAA bilayer growing process ( $\lambda_{\text{exc}}$  480 nm). The numbers 1–5 correspond to the first through fifth CS/PTAA bilayers.

The fluorescence spectra were recorded using a Spex Fluorolog 1680 spectrophotometer. A Perkin-Elmer UV–vis–near-IR spectrometer, Lambda 900, using a quartz cuvette of 1 cm path length, measured the UV–vis absorption spectra of the solutions. An epifluorescence microscope (Olympus IX-FLA) was used for acquiring the epifluorescence micrographs. A thermoelectrically cooled Optronics Magnafire TMCCD camera detected the emission of the adsorbed layers.

**2.1.1. Preparation of the Quartz Slide.** The quartz slides were rinsed in a detergent solution to remove any impurities from the surface. This was followed by sonication in pure water for 30 min to remove detergent from the slide. The slide was then made hydrophilic using the RCA method.<sup>43</sup> The slides were then sonicated with pure water.

**2.1.2. Immobilization of Polyelectrolytes onto the Quartz Slide.** The negatively charged quartz slide was alternately immersed in aqueous solutions of oppositely charged CS (positive) and PTAA (negative) polyions for 10 min.<sup>48</sup> Each immersion was followed by washing the slide in a buffered solution which had the same pH as the dipping solution, as described in section 2.1. For each cycle, a bilayer film of CS/PTAA was formed on both sides of the slide. The slide was dried with a cool stream of air. The fluorescence spectrum of the quartz slide was recorded in air after each assembly cycle. This cycle procedure was repeated five times until a stable film was obtained. After the bilayer system of CS and PTAA (five bilayers) was built, the slide was immersed in a beaker of water for 20 min to determine whether the film would be washed away. The fluorescence spectrum of the slide was again recorded and compared to the recorded spectrum of bilayer 5 to determine this. On top of this stable bilayer system, two bilayers of OPH/PTAA were deposited by alternately immersing the slide in aqueous solutions of OPH and PTAA for 10 min. On top of the OPH/PTAA bilayers one last layer of OPH was adsorbed. This multilayer system of CS, PTAA, and OPH from now on referred to as a *sensor* was used for the detection of paraoxon.

### 3. Results and Discussion

**3.1. Fluorescence Emission Spectroscopic Studies of the LbL Adsorbed Films.** The optical property fluorescence of PTAA was used as a reference to monitor the growth of the CS/PTAA binary system. PTAA solution has a  $\lambda_{\text{max}}$  at 575 nm (Figure 1). The fluorescence spectra showed a shift toward the red region for the CS/PTAA bilayers that were adsorbed onto

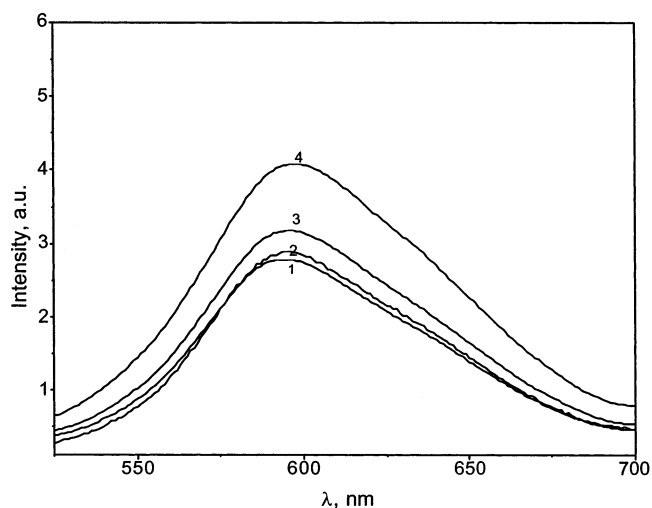


**Figure 2.** Fluorescence spectra of the growing OPH/PTAA bilayer system that was added on top of the fifth CS/PTAA bilayer system ( $\lambda_{\text{exc}}$  480 nm): (1) fifth CS/PTAA bilayer before deposition of OPH/PTAA, (2) first OPH/PTAA bilayer, (3) second OPH/PTAA bilayer, (4) top OPH layer.

the quartz slide due to the formation of aggregates.<sup>52</sup> The fluorescence intensity band at  $\lambda_{\text{max}}$  600 nm was seen for each fluorescence spectrum that was taken. This single band at  $\lambda_{\text{max}}$  600 nm corresponds to the presence of the PTAA layers. The increasing intensity of the fluorescence spectra confirms the growth of the bilayer system by the LbL deposition technique. The fluorescence intensity does not change dramatically between the fourth and fifth bilayers, and at this point a homogeneous film was noted.

After five bilayers of CS/PTAA were built, the stability of this system was tested by placing the quartz slide in pure water for 20 min. The fluorescence measurement showed no significant change in intensity. This verified that the five-bilayer ultrathin film was sufficiently stable due to the strong electrostatic forces between the oppositely charged layers, and further deposition of CS/PTAA bilayers was unnecessary.

The OPH/PTAA bilayers continued the growth of the multilayer system, and this was also followed using fluorescence spectroscopy (Figure 2). Two bilayers of OPH/PTAA were adsorbed onto the ultrathin film of CS/PTAA that provided an independent interface for the immobilization of OPH. A layer of OPH was adsorbed as the last layer of the system to be able to detect paraoxon. The fluorescence spectrum was recorded after the last layer of OPH was added, and this was used as the reference for further comparison of the substrate after exposure to paraoxon.

The sensor was placed in a small beaker containing an aqueous paraoxon solution ( $10^{-9}$  M) for 1 min, removed, and dried with a cool stream of air, and the fluorescence spectrum of the sensor was recorded. This was repeated several times with increasing concentrations of paraoxon solution. The fluorescence intensity of the sensor after exposure to paraoxon solution decreased with increasing concentrations of paraoxon solution (Figure 3). This decrease in fluorescence intensity is explained by the fact that the PTAA layer is sandwiched

(51) Guilbault, G. In *Analytical Uses of Immobilized Enzymes*; Guilbault, G., Eds.; Marcel Dekker: New York, 1984.

(52) McRae, E.; Kasha, M. In *Physical Processes in Radiation Biology*; Augenstein, L., Mason, R., Rosenberg, B., Eds.; Academic Press: New York, 1964.



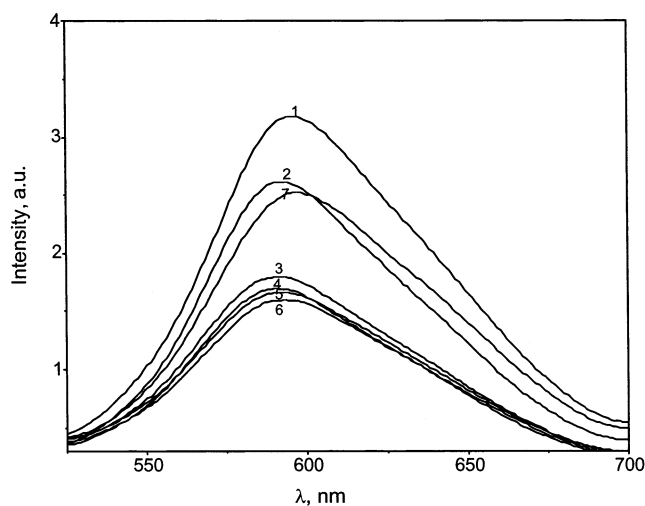


**Figure 3.** Fluorescence spectra of OPH in the presence of different concentrations of aqueous paraoxon solution ( $\lambda_{\text{exc}}$  480 nm): (1) top layer of OPH, (2)  $1 \times 10^{-9}$  M, (3)  $1 \times 10^{-8}$  M, (4)  $4 \times 10^{-8}$  M, (5)  $8 \times 10^{-7}$  M, (6)  $0.5 \times 10^{-6}$  M, (7) recovery of enzyme after the sensor was left overnight in  $\text{KH}_2\text{PO}_4/\text{NaOH}$  buffer.

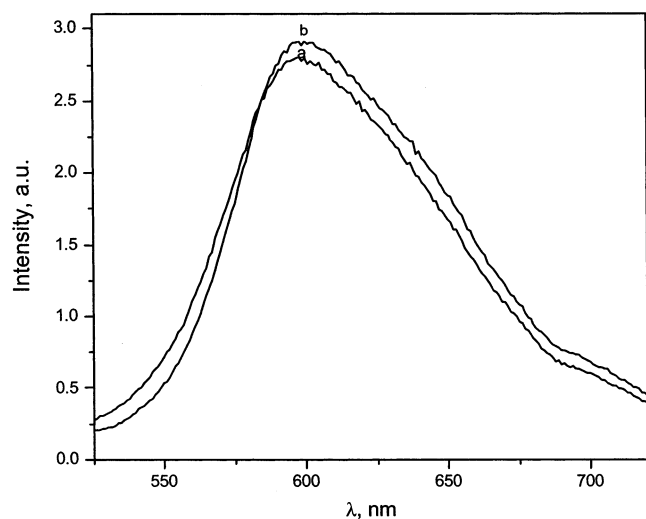


**Figure 4.** Fluorescence spectra of the CS/PTAA system in the absence of OPH used to prove that OPH is responsible for the paraoxon detection ( $\lambda_{\text{exc}}$  480 nm): (a) fifth bilayer of CS/PTAA, (b)  $10^{-6}$  M paraoxon solution.

between two layers of OPH, i.e., one layer of OPH on both sides of the PTAA layer. Any interaction of the OPH layer with paraoxon will cause a change of conformation of the enzymes forming the layer, which causes the PTAA molecules to aggregate. Recovery of the activity of the enzyme after the sensor is washed in  $\text{KH}_2\text{PO}_4/\text{NaOH}$  buffer will favor the recovery of the enzyme conformation and as a consequence a partial disaggregation of the PTAA molecules, which explains the increase of the intensity of fluorescence (Figure 3, spectra 6 and 7). The sensor could be recovered and can be reused for the detection of at least 10 samples of paraoxon.

A reference quartz slide was prepared on which five bilayers of CS/PTAA were adsorbed. The results observed are shown in Figure 4. The results indicate that in the absence of OPH there is marginal change in the fluorescence intensity spectra from the fifth CS/PTAA bilayer to that in the presence of paraoxon. This proves that OPH is responsible for the hydrolysis of paraoxon.

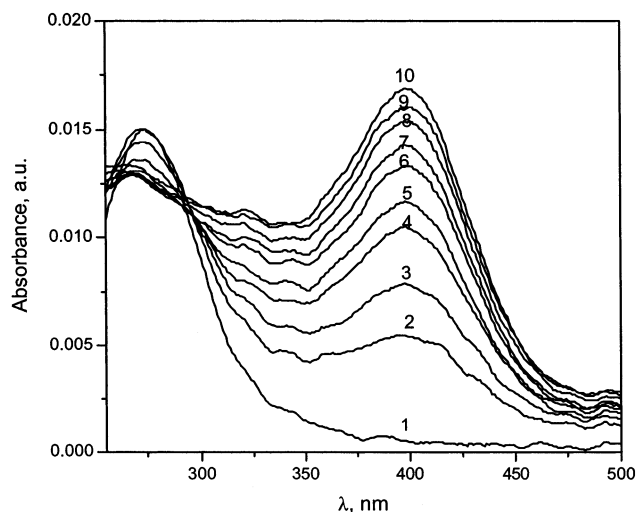


**Figure 5.** UV-vis absorption spectra of the hydrolysis product PNP at different time intervals for the detection of paraoxon solution: (1) paraoxon solution ( $8 \times 10^{-7}$  M). Incubation time of the substrate in paraoxon solution: (2) 30 s, (3)–(10) 1, 2, 3, 4, 5, 6, 8, 9, and 10 min.

### 3.2. UV-Vis Absorption Studies for the Detection of Paraoxon Using LbL Adsorbed Films.

One method used to illustrate that the LbL adsorbed films successfully works for the detection of paraoxon is the UV-Vis absorption spectrum of *p*-nitrophenol (PNP). OPH hydrolyzes the phosphotriester bond of paraoxon, releasing the hydrolysis products, one of which is PNP ( $\lambda_{\text{max}}$  400 nm). In this experiment, an aqueous solution of paraoxon ( $8 \times 10^{-7}$  M) was placed in a quartz cuvette and the UV-Vis spectrum was recorded. As seen in Figure 5, paraoxon has a  $\lambda_{\text{max}}$  at 274 nm. After the absorption spectrum of the paraoxon solution was recorded, the sensor was placed in the quartz cuvette for different time intervals. After the initial exposure of the sensor to the paraoxon solution for 30 s, the sensor was removed and the UV-Vis absorption spectrum of the solution in the quartz cuvette was recorded. Figure 5 shows that, after exposure of the paraoxon solution in the cuvette to the immobilized OPH, the absorption spectrum showed a new  $\lambda_{\text{max}}$  at 400 nm (curve 2). This corresponds to the hydrolysis product PNP. The sensor was again placed in the cuvette for another 30 s so that the solution was exposed to the enzyme for 1 min. The sensor was again removed, and the UV-Vis spectrum was recorded (curve 3). The procedure of exposing the paraoxon solution to the sensor was repeated several times until the total time that the paraoxon solution was exposed to the sensor was 10 min. Figure 5 shows that the  $\lambda_{\text{max}}$  at 274 nm decreases with a corresponding increase in the  $\lambda_{\text{max}}$  at 400 nm as the exposure time increases. The isosbestic point at 292 nm at the beginning of the hydrolysis (Figure 5, curves 2–7) confirms that there is a transition from the paraoxon to the hydrolyzed product. The initial increase in the  $\lambda_{\text{max}}$  at 400 nm is steep as compared to the absorption band after 2 min (Figure 5, curve 4). The rapid activity of the enzyme system is shown by the presence of the absorption band for PNP within as little as 30 s. UV-vis spectroscopy shows that paraoxon is successfully degraded by the immobilized OPH, releasing less toxic products, one of which is PNP. Lower concentrations of paraoxon can also be detected, but they need a longer incubation time of the sensor in the paraoxon solution for a measurable quantity of PNP to be produced. This sensor

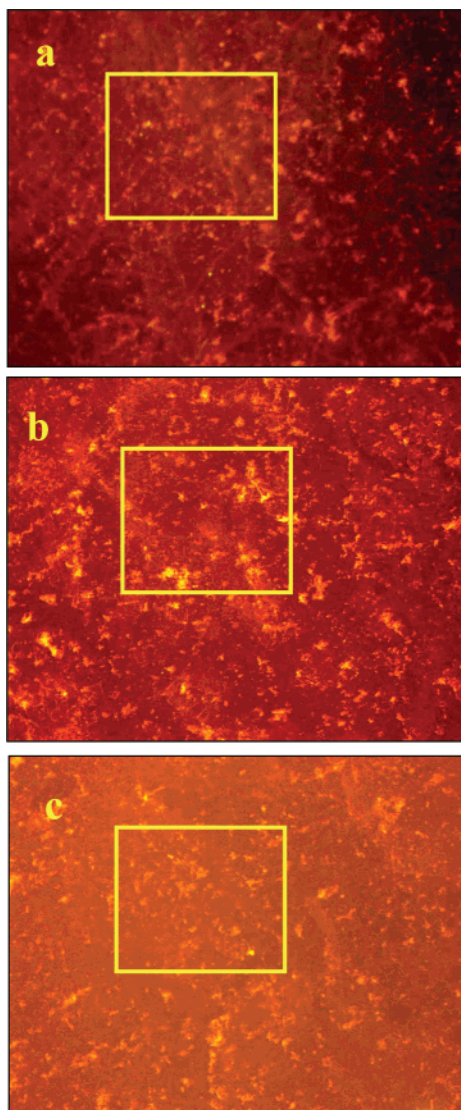


**Figure 6.** Epifluorescence microscope images of the bilayer system: (a) fifth bilayer of CS/PTAA, (b) multilayer from (a) plus two bilayers of OPH/PTAA and one OPH layer, (c) substrate from (b) after exposure to  $10^{-9}$  M paraoxon for 1 min. Image size  $895 \mu\text{m} \times 713 \mu\text{m}$ .

is very sensitive because concentrations as low as  $10^{-9}$  M paraoxon can be detected.

**3.3. Epifluorescence Microscopy Studies of the LbL Adsorbed Films.** The epifluorescence microscopy studies applied to the adsorbed layers provide a versatile method to visually observe the topography of these self-assembled layers and are also used to confirm the formation of aggregates. An epifluorescence microscope image taken after the fifth bilayer of CS/PTAA showed some bright orange spots, which illustrate the fluorescent CS/PTAA system (Figure 6a). This was compared to the epifluorescence microscope image taken after the PTAA/OPH bilayers were deposited, and there was a change in the topography (Figure 6b) shown by the increase in size of the fluorescent orange spots.

After exposure of the substrate to paraoxon solution for 1 min, the epifluorescence image was again taken, and there was an additional change (Figure 6c). The intensity of the bright orange spots dramatically decreases, and we attributed this fading phenomenon to the nonfluorescent PNP molecules. These results support what was illustrated from fluorescence spectroscopy. Exposure of the substrate to paraoxon causes a change in conformation of the enzymes, leading to a corresponding change in the PTAA aggregate state and hence fluorescent quenching.

#### 4. Conclusion

From these studies, we can conclude that the assembly of CS/PTAA can be successfully prepared by alternate layer-by-layer deposition on a quartz slide. This stable ultrathin film provides a well-defined substrate-independent interface for enzyme immobilization, in which the bioactivity of OPH is not compromised. This leads to fast detection of paraoxon and quick recovery times. The spectroscopic and microscopic methodologies used suggest that nonfluorescent aggregates are formed. The multilayer system has the advantage of being simple, fast, and reproducible.

**Acknowledgment.** This work was supported by a grant from the U.S. Army Research Office under Contract DAAD19-00-1-0138.

JA028691H